

# Two-Point Temperature Control Structure Selection for Dividing-Wall Distillation Columns

Kwangil Kim,<sup>†</sup> Moonyong Lee,<sup>\*,‡</sup> and Sunwon Park<sup>\*,†</sup>

<sup>†</sup>Department of Chemical and Biomolecular Engineering, Korea Advanced Institute of Science and Technology, Taejeon, Korea

<sup>‡</sup>School of Chemical Engineering, Yeungnam University, Dae-dong, Kyeongsan 214-1, Korea

## Supporting Information

**ABSTRACT:** Two-point temperature control structures of dividing-wall columns (DWCS) were investigated to overcome difficulties arising from their complicated natures. The control performance of DWCS was assessed for nine different feed conditions characterized by the composition of an intermediate component and their relative volatility. Steady-state and dynamic simulations were performed to analyze the closed-loop responses for various two-point temperature control structures of DWCS. It is shown that proper control strategies depend strongly on feed characteristics, particularly on the relative volatilities of the feed components. Control structure evaluations follow from the rigorous simulations, and basic guidelines for selecting proper control structures for DWCS are proposed in relation to the feed conditions.

## 1. INTRODUCTION

Distillation plays an important role in chemical process industries and consumes the largest amount of energy among existing separation processes. The huge impact of distillation processes on both operating and investment costs has motivated the development of various types of fully thermally coupled distillation columns. The dividing-wall column (DWC) arrangement is one of the most popular thermally coupled distillation implementations for the separation of ternary mixtures. By avoiding remixing problems, DWCS can significantly reduce energy consumption with respect to that of conventional distillation sequences.<sup>1–10</sup> Furthermore, an overall reduction in capital costs can also be expected through the elimination of a column shell, reboiler, and condenser.

Despite the potential benefits of DWCS, a relatively limited number of such columns have been implemented in the field. Since Wright<sup>11</sup> first introduced the concept of the DWC in 1949, just over 90 commercial-scale applications have been reported.<sup>12</sup> This slow acceptance of DWCS in the process industry has partly been attributed to their difficult control properties resulting from their highly coupled complex structures.<sup>13</sup>

To address control issues, research into the operation, control, and controllability of DWCS has been actively conducted: Wolff and Skogestad<sup>14</sup> considered the operation and control of DWCS. They did not find significant problems with the (*L*, *S*, *V*) composition control scheme where the top, side, and bottom product compositions are controlled by manipulation of the reflux flow rate (*L*), side draw rate (*S*), and boilup flow rate (*V*), respectively. Annakou et al.<sup>15</sup> analyzed a heat-integrated two-column system and a DWC for the separation of ternary mixtures. They used degree-of-freedom analysis and steady-state control structure synthesis to find that these systems could be controlled by conventional decentralized control structures. Mutalib and Smith<sup>16</sup> studied the operation and control of DWCS, considering two control structures: (*L*, *S*, *V*) and (*D*, *S*, *V*), where *D* represents the distillate flow rate. Hernández and Jiménez<sup>17</sup> compared the dynamic properties of a column with a side

rectifier, a column with side strippers, and a Pelyuk system. They found the Pelyuk system to be the most energy-efficient, but the column with a side rectifier gave the best dynamic results. Serra et al.<sup>18</sup> investigated the controllability of different control structures and the effects of operation optimality on the controllability of DWCS. They showed that the (*D*, *S*, *B*) pairing (where *B* represents the bottoms flow rate) provides good dynamic responses. Adrian et al.<sup>19</sup> applied model-predictive control to DWCS and found this approach to be suitable for integrated and strongly coupled processes such as DWCS. Hernández et al.<sup>20</sup> compared the feedback control behaviors of five thermally integrated distillation schemes and conventional distillation schemes and found that the Pelyuk column provided the best dynamic performance at high levels of intermediate component. Cho et al.<sup>21</sup> proposed a profile position control scheme to obtain desired column profiles of DWCS. They applied this technique to a benzene–toluene–xylene separation and confirmed that tight control of the profile position could give a stable separation in DWCS.

Although recent publications have reported considerable advances in control strategies in DWCS, most of these works investigated a specific feed mixture, so the results were restricted to that particular feed rather than a general feed. In fact, once a required product purity is given, the optimal control structure of a DWC largely depends on the feed characteristics. Thus, it still remains unclear how the performance of a control strategy is affected by the feed characteristics.

Also, previous reports have mostly been concerned with three-point control, which controls compositions or temperatures at three different points of the column simultaneously. In practice, however, because of difficulties and high maintenance costs in composition measurement, temperature control is preferred

**Received:** June 8, 2012

**Revised:** October 6, 2012

**Accepted:** November 7, 2012

**Published:** November 7, 2012

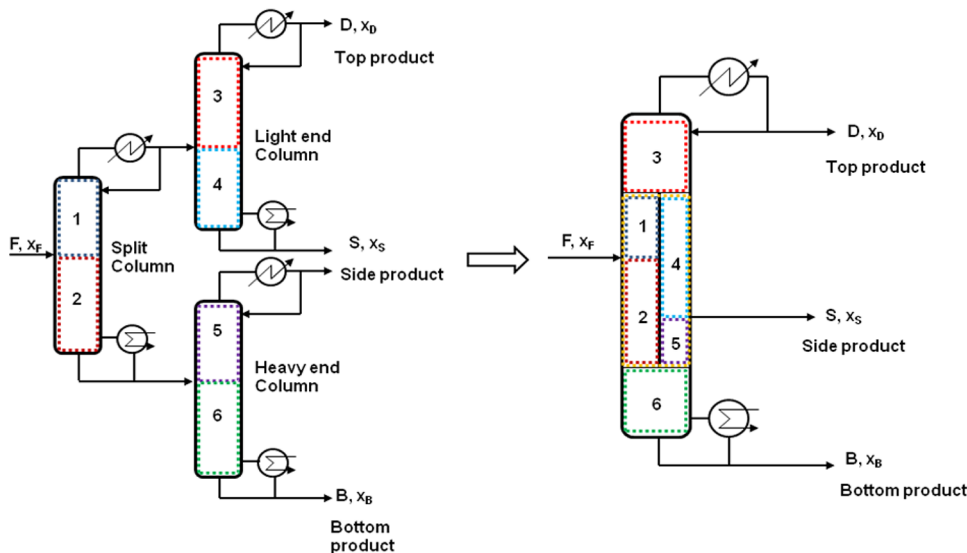


**Figure 1.** Schematic diagram of the sloppy column configuration and DWC.

rather than direct composition control. Furthermore, practical problems with three-point control could arise from strong process interactions between controlled variables that might accompany significant performance degradation and instability.

For this reason, as long as the composition offset is in a reasonable range, a two-point control structure can be an attractive practical option in DWC control to mitigate the process interaction effect. Mutalib and Smith<sup>22</sup> proposed several two-point temperature control structures and investigated control performance using a pilot plant. They concluded that two-point temperature control structures could control the product purity of a DWC successfully within a reasonable offset range. To minimize the product purity offset, various techniques such as over-refluxing or multiple temperature measurements have also been proposed.<sup>23–25</sup>

In this article, various two-point temperature control structures are studied for the control of DWCs. The feed mixtures belonging to ideal solutions are evaluated and classified into nine representative cases based on the relative volatilities and compositions of the key components. To investigate proper control strategies with respect to feed conditions, both steady-state and dynamic analyses are examined for each feed mixture case. General DWC control guidelines are finally proposed in terms of feed characteristics.

## 2. DESIGN AND SIMULATION OF A DWC

A shortcut design procedure<sup>26</sup> based on a sloppy column configuration shown in Figure 1 is applied for the initial design of the DWC structure. As seen from the figure, the prefractionation section and the upper and lower parts of the main fractionation section in the DWC are equivalent to the split column and the light and heavy end columns, respectively, in the sloppy configuration.

Nine different feed mixtures were used to investigate the effects of feed composition and relative volatilities of the feed mixtures. Three feed compositions were considered to investigate the effect of key component composition: a mixture with low amounts of the intermediate component (F1), an equimolar mixture (F2), and a mixture with high amounts of the intermediate component (F3). Three mixtures were also considered to assess the effects of relative volatilities in terms

of the ease of separability index (ESI),  $\text{ESI} = \alpha_{A-B}/\alpha_{B-C}$ ,<sup>27</sup> where  $\alpha$  denotes a relative volatility between the two key components. By definition, for  $\text{ESI} < 1$ , the A/B split is harder than the B/C split, whereas for  $\text{ESI} > 1$ , the A/B split is easier than the B/C split, where A, B, and C denote the light, intermediate, and heavy components, respectively. The mixtures were chosen based on those studied by Jiménez et al.<sup>3</sup> and are listed in Table 1. The

**Table 1.** Feed Mixtures Used in the Simulation Study

components	F1	F2	F3
Mixture M1 (ESI = 1.04)			
<i>n</i> -pentane (A)	0.4	0.33	0.2
<i>n</i> -hexane (B)	0.2	0.33	0.6
<i>n</i> -heptane (C)	0.4	0.33	0.2
Mixture M2 (ESI = 1.86)			
<i>n</i> -butane (A)	0.4	0.33	0.2
<i>i</i> -pentane (B)	0.2	0.33	0.6
<i>n</i> -pentane (C)	0.4	0.33	0.2
Mixture M3 (ESI = 0.47)			
<i>i</i> -pentane (A)	0.4	0.33	0.2
<i>n</i> -pentane (B)	0.2	0.33	0.6
<i>n</i> -hexane (C)	0.4	0.33	0.2

feed, in the vapor state, was introduced onto the column at a flow rate of 45 kmol/h at 1 atm. The specifications of product purity were selected as 99%, 94%, and 99% for the distillate, intermediate, and bottom products, respectively. Thermodynamic properties were computed using the Peng–Robinson equation of state. The resulting DWC structures are also summarized in Table 2.

The process simulator HYSYS was employed for the simulation and design of all cases. For the implementation of a DWC in the HYSYS environment, the Petlyuk column configuration was used because it is thermodynamically equivalent to a DWC. The resulting process flow diagram of a DWC for the HYSYS simulation is shown in Figure 2.

In practice, depending on the operation situation, temperature control loops are often changed to a manual mode from an automatic mode or vice versa. Thus, a desirable control scheme must provide automatic regulation of the material balance in any operating mode. In this study, according to this popular guideline

Table 2. Results of DWC Structure Design

	F1M1	F1M2	F1M3	F2M1	F2M2	F2M3	F3M1	F3M2	F3M3
prefractionator <sup>a</sup>	8	10	11	7	10	11	6	9	10
feed stream <sup>b</sup>	3	5	5	4	5	5	3	5	4
main column <sup>a</sup>	31	65	59	31	63	58	31	63	59
side stream <sup>c</sup>	15	19	47	15	17	46	14	16	46
dividing wall <sup>c</sup>	6, 25	4, 45	20, 57	6, 24	4, 40	23, 56	8, 22	6, 34	28, 55

<sup>a</sup>Number of stage. <sup>b</sup>Stage location based on prefractionator. <sup>c</sup>Stage location based on main column.

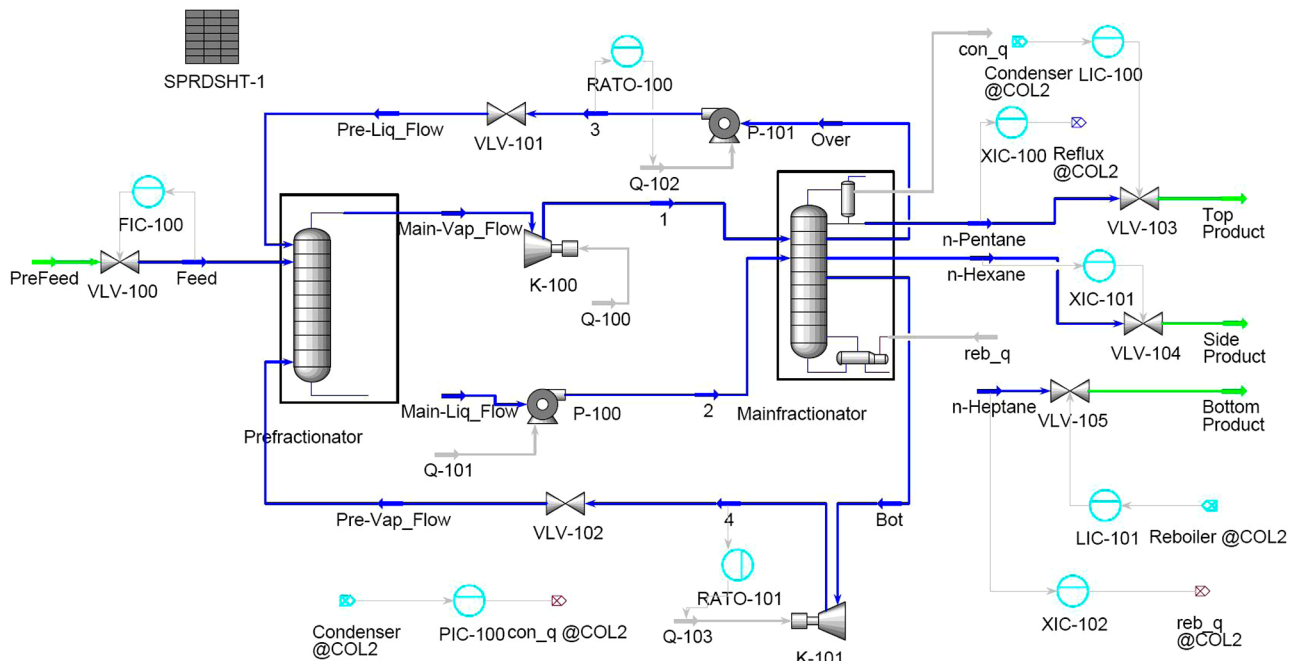


Figure 2. Process flow diagram of a DWC in HYSYS.

in practical distillation control, the distillate flow rate ( $D$ ) and bottoms flow rate ( $B$ ) were assigned to the condenser and reboiler liquid level control, respectively. Accordingly, the manipulated variables for temperature control were restricted to the reflux flow rate ( $L$ ), side draw rate ( $S$ ), and boilup flow rate ( $V$ ). This scheme is also reported to be the most commonly used scheme for one-point control of conventional distillation columns in practice.<sup>28</sup>

### 3. SENSOR LOCATION FOR TWO-POINT TEMPERATURE CONTROL

**3.1. Steady-State Gain Analysis.** Incremental changes in the column temperature profile were analyzed for typical manipulated variables in order to choose the location for temperature measurements in the DWC. For this analysis,  $L$ ,  $S$ , and  $V$  were considered as the possible manipulated variables for temperature control, and  $D$  and  $B$  were assigned for inventory control. The liquid split ratio ( $R_L$ ) and vapor split ratio ( $R_V$ ) into the dividing-wall section were fixed during design of the DWC. For linearity, the step changes of  $L$ ,  $S$ , and  $V$  were of sufficiently small magnitude ( $\pm 0.05\%$  of the steady-state value). Figure 3 shows the steady-state gain profiles based on the average temperature deviation values for increasing and decreasing step changes in  $L$ ,  $S$ , and  $V$  in the nine feed cases.

When the ESI value was close to 1 (the M1 cases), two apparent peaks occurred in the steady-state gain profile around the end of the dividing-wall section for step changes of  $L$  and  $V$ .

For a step change of  $S$ , only one apparent peak occurred (except for the F1M1 case) in the steady-state gain profile around the low end of the dividing-wall section. Changes in the internal liquid flows achieved by changing  $S$  directly influence the vaporized heavy components in the stripping section but do not directly affect the vapor flow in the rectifying section, which contains mainly light and intermediate components. For this reason, the step change of  $S$  mainly affected the temperature of the stages below the side draw stage.

Separation of a mixture with a large ESI value normally requires a pinch zone in the column's bottom section to separate the intermediate and heavy components. On the other hand, the separation of light and intermediate components is relatively easy and thus no pinch zone in the upper section is required. Therefore, when the ESI value was large (the M2 cases), one apparent peak normally occurred in the steady-state gain profile around the upper end of the dividing-wall section for  $L$  and  $V$  changes. Consequently, the steady-state gains of the lower stages were not significant, whereas those of the upper stages were apparent, as seen from Figure 3. For a step change of  $S$ , a peak in steady-state gains occurred around the low end of the dividing-wall section because it mainly affected the temperature of the stages below the side draw stage, as mentioned before.

When the ESI value was small (the M3 cases), the main column had a pinch zone in the upper section because of the difficulty in separating light and intermediate components. Therefore, temperature changes or gains of the lower stages were

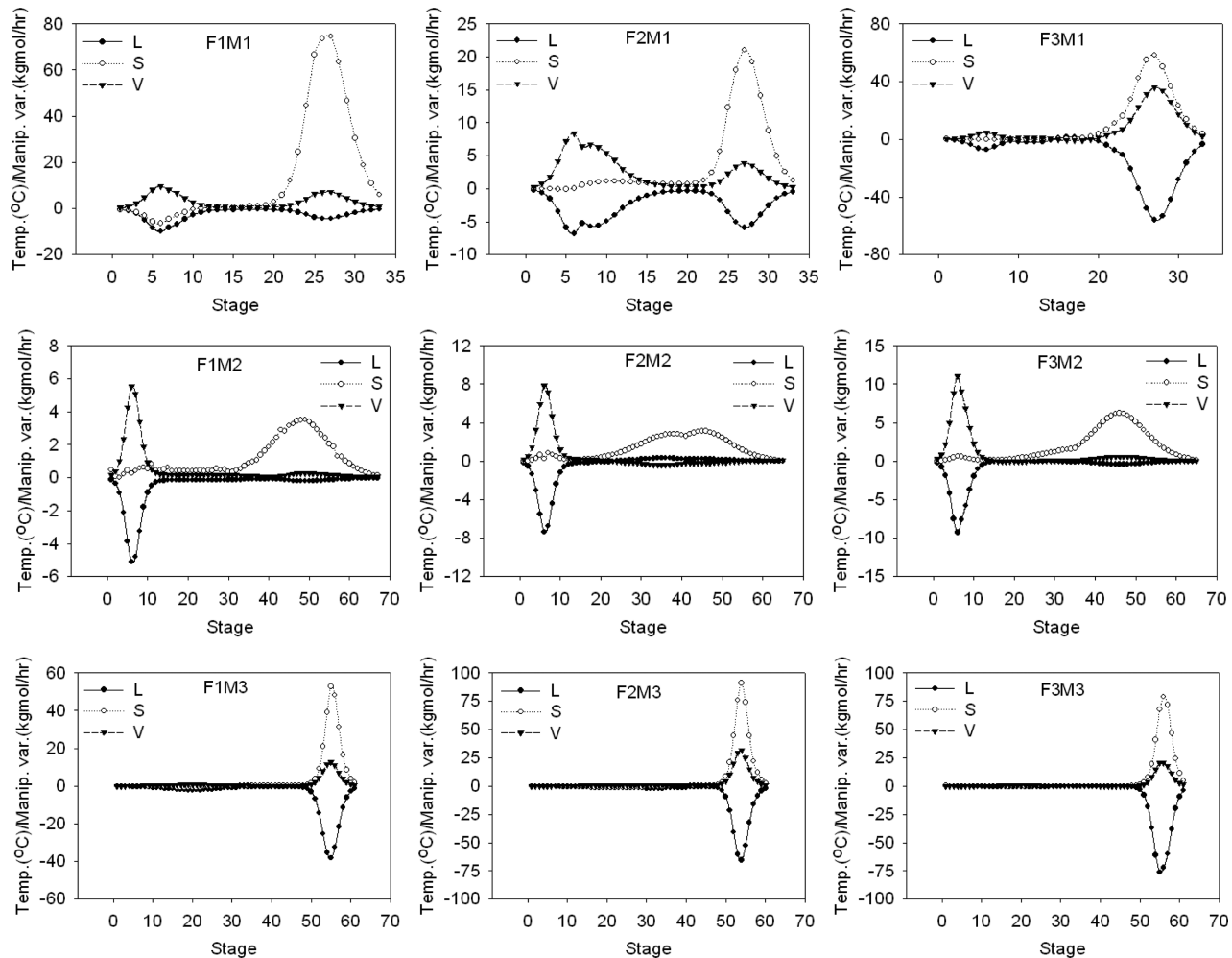


**Figure 3.** Steady-state gain plots for step changes of  $L$ ,  $S$ , and  $V$  in the nine feed cases.

significant compared to those of the upper stages, resulting in one apparent peak in the steady-state gain profile around the low end of the dividing-wall section for  $L$  and  $V$  changes. The peak in the steady-state gain profile also occurred around the low end of the dividing-wall section for a step change of  $S$ . For the M3 cases, no manipulated variables showed apparent effects on the temperature of the column's upper stages. Therefore, in the M3 cases, controlling the temperature of the upper stages was expected to be difficult because of this insensitivity.

For two-point temperature control, two positions should first be determined for temperature control. From the steady-state sensitivity point of view, the stages at the two peaks in the steady-state gain profile are good candidates for two-point temperature control. However, for some cases (particularly the M3 cases), it is still unclear from the steady-state gain analysis which stages have to be chosen for temperature control. This situation requires further analysis by other methods to find the proper stages for two-point temperature control.

**3.2. Singular Value Decomposition (SVD) Analysis.** Selecting sensor locations for multivariable control requires balancing the effects of sensor interaction and loop sensitivity. Singular value decomposition (SVD) provides a basis for further analysis to identify unclear sensor locations in the gain matrix.<sup>29</sup> In the SVD analysis, a steady-state gain matrix is decomposed into three unique component matrices

$$\mathbf{K} = \mathbf{U}\Sigma\mathbf{V}^T \quad (1)$$

where  $\mathbf{K}$  is the steady-state gain matrix,  $\mathbf{U}$  and  $\mathbf{V}$  are the orthonormal matrices (the columns of which are called the left and right singular vectors, respectively), and  $\Sigma$  is a diagonal matrix of singular values. The  $\mathbf{U}$  matrix is important in selecting the best sensor location: The sensor location should be chosen to give the largest absolute value in each of the columns of the  $\mathbf{U}$  matrix.

In this work, SVD analysis was applied for three possible configurations:  $L-S$ ,  $L-V$ , and  $S-V$ . The names of the configurations are based on the manipulated variables used to control either the upper- or lower-stage temperatures. For example, the  $L-S$  configuration means that one of the two temperature sensor stages is controlled through either  $L$  or  $S$  and the other stage through the other remaining manipulated variable. Figure 4 shows plots of the  $\mathbf{U}$  vectors from the SVD analysis in the  $L-S$  configuration as an example. The  $\mathbf{U}$  vectors in the figure clearly show which stages are most sensitive in a given configuration. For example, the most sensitive regions of the F1M1 case are between stages 5 and 7 and between stages 25 and 29.

The  $\mathbf{U}$  vectors in the M1 cases have larger magnitudes than those in the M2 or M3 cases, indicating that the M1 cases give the most sensitive temperature changes over the whole column. In the M2 cases, the column's upper section shows sensitive temperature changes because of the relatively easy separation of the light and intermediate components. The M3 cases show

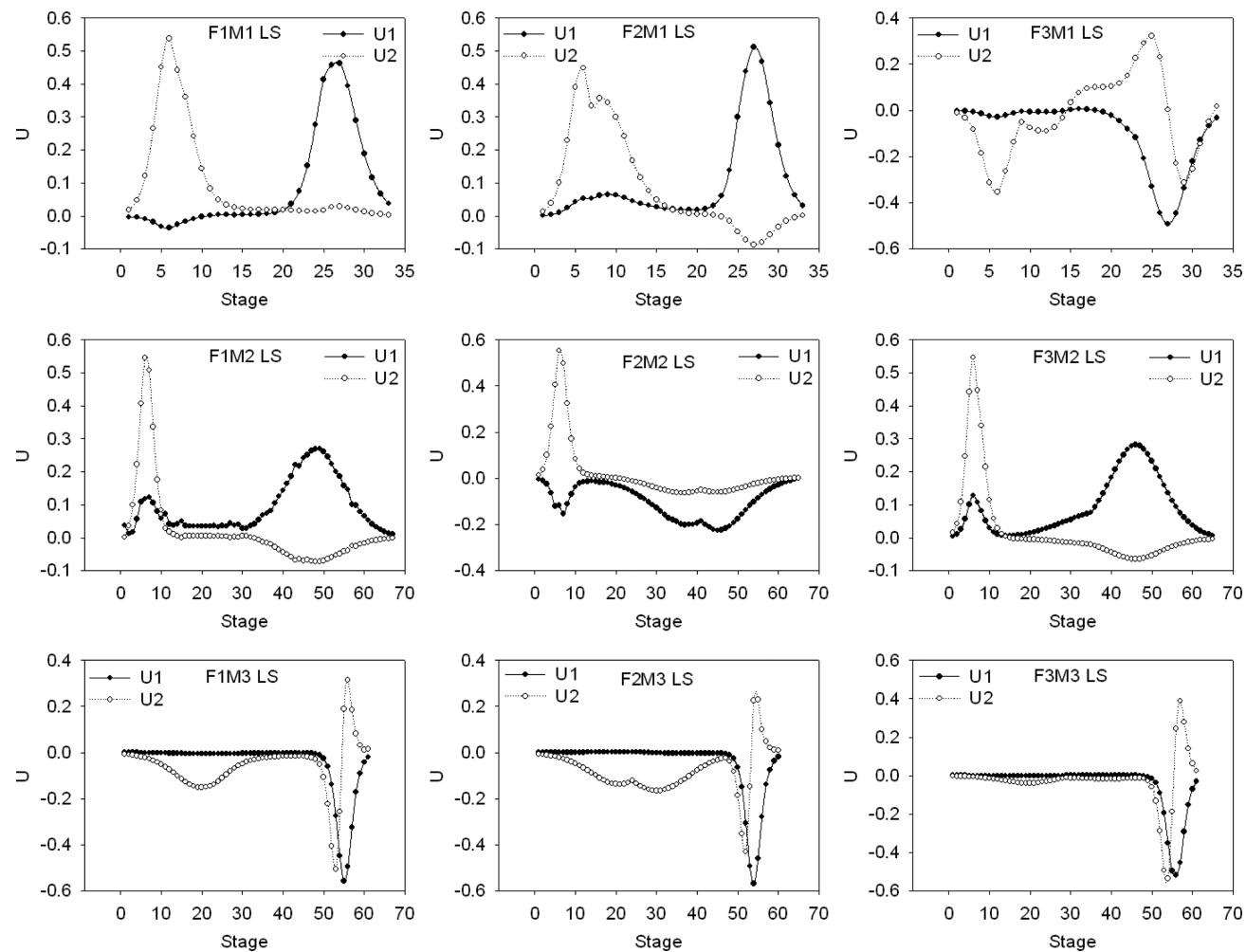


**Figure 4.** U vector plots of the L-S configuration.

**Table 3. Selected Sensor Locations for the L-S, L-V, and S-V Configurations**

	L-S			L-V			S-V		
	F1	F2	F3	F1	F2	F3	F1	F2	F3
M1	6, 26	6, 27	6, 23	8, 27	6, 27	6, 27	6, 25	9, 25	6, 23
M2	7, 43	7, 49	9, 49	8, 49	7, 45	6, 47	7, 43	7, 45	7, 48
M3	21, 57	29, 54	21, 55	20, 54	35, 54	21, 55	21, 55	29, 54	23, 56

behavior opposite that of the M2 cases, with most sensitivity in the lower section because separation of heavy and intermediate components is relatively easy. In the nine feed cases, the most sensitive sections were commonly located near interlinking stages between the prefractionator and the main column, that is, the end of dividing-wall section. Note that sensor locations of the upper stages for the M3 cases, which were unclear in the steady-state gain matrix, were clearly distinguished in the SVD analysis. The SVD analysis was also carried out for the L-V and S-V configurations. Table 3 lists the sensor stages selected from the SVD analysis for all three possible configurations.

#### 4. STEADY-STATE ANALYSIS FOR CONTROL STRUCTURE SCREENING

**4.1. Relative Gain Array (RGA) Analysis.** The relative gain array (RGA)<sup>30</sup> technique can be used for analyzing the interactions between control loops to screen the undesirable pairing alternatives. The results of RGA analysis are summarized

in Table 4 for possible control configurations. The RGA results for the L-S configuration consistently indicate that the temperature of the upper stage should be controlled by L and the lower stage by S. The RGA results for the S-V configuration consistently show that the temperature of the upper stage should be controlled by V and the lower stage by S. Control of the upper-stage temperature by manipulation of V might be possible in practice because any change in vapor flow can be transferred up to the upper section quickly, compared to the transfer of liquid flow changes down to the lower section. In the L-V configuration, RGA analysis recommends that the temperature of the upper stage should be controlled by L and the lower stage by V, except for the F2M1, F2M2, and F3M3 cases, for which the reverse pairing is suggested.

**4.2. Singular Value Decomposition (SVD) Analysis.** The pairing that will most closely approximate the SVD decoupler and yield the least open-loop interaction is one in which the sensor associated with the largest component of the U1 column

**Table 4.** Relative Gain Array Results for the L-S, L-V, and S-V Configurations

	L-S			L-V			S-V		
	F1	F2	F3	F1	F2	F3	F1	F2	F3
M1	0.963	0.037	1.003	-0.003	0.973	0.027	2.494	-1.494	-1.159
	0.037	0.963	-0.003	1.003	0.027	0.973	-1.494	2.494	-1.159
M2	1.003	-0.003	0.992	0.008	1.005	-0.005	6.017	-5.017	-2.815
	-0.003	1.003	0.992	0.008	1.005	-0.005	5.017	6.017	3.815
M3	0.779	0.221	0.670	0.330	0.630	0.370	1.862	-0.862	11.54
	0.221	0.779	0.330	0.670	0.370	0.630	-0.862	1.862	-10.54

vector is paired with the manipulated variable associated with the largest component of the **V1** column vector.<sup>31</sup> The largest component of the **U2** vector should also be paired with the largest component of **V2**. The SVD results for the L-S, L-V, and S-V configurations are listed in Tables 5–7, respectively. The recommended loop pairings for the L-S and S-V configurations are consistent with those recommended by the RGA analysis. However, the pairing results for the L-V configuration disagree with the results from the RGA analysis for all feed cases, except for the F2M1, F2M2, and F3M3 cases. When the pairings by the RGA and SVD analyses conflict with each other, the proper choice depends on the situation. For this reason, it is good practice to consider both RGA and SVD analyses when examining controller pairings. There are two problems that lead to conflicting RGA and SVD results.<sup>31</sup> First, conflicted pairings can result when the system has a high condition number because loop pairing by RGA analysis does not consider the condition and sensitivity of the multivariable system. Another problem is that SVD analysis addresses only the open-loop nature of the system and recommends controller pairing that will give the control system the greatest open-loop advantage in terms of loop sensitivity and loop interaction. It does not consider the closed-loop “decommissioning” problem, which is addressed by RGA.

#### 4.3. Condition Number (CN) and Niederlinski Index (NI)

**Analyses.** The condition number (CN) is generally defined as the ratio of the largest singular value to the smallest singular value.<sup>29</sup> For dual-ended control problems, it is defined as the ratio of the first and second singular values:  $CN = \sigma_{\text{largest}}/\sigma_{\text{smallest}} = \sigma_1/\sigma_2$ . The condition number provides a numerical indication of the balance of sensitivities in a multivariable system. Low condition numbers indicate that multivariable gains are well balanced and thus result in a system with sufficient degrees of freedom to meet the dual-ended control objectives. High condition numbers suggest an imbalance in the multivariable gains. Imbalance signifies when the column is much more sensitive in one vector direction than it is in the other. The CN values calculated for all feed cases and control configurations are listed in Table 8, where it can be seen that all of the M3 cases showed high CNs regardless of control configurations. The M2 cases and the F3M1 case also indicated high CNs for the L-V configuration. It should be noted that, in the L-V configuration, the loop pairings obtained by the SVD and RGA analyses turned out to conflict with each other for most of these ill-conditioned cases.

The Niederlinski index (NI)<sup>32</sup> can be used to eliminate unworkable pairings of variables at an early stage in the design. The controller settings do not have to be known, but the NI applies only when integral action is used in all loops. It uses only the steady-state gains of the process transfer function matrix. The method employs a necessary but not sufficient condition for the stability of a closed-loop system with integral action. If the index is positive, the system might or might not be stable. If the index is negative, the system will have “integral instability” for any controller settings, and thus, the corresponding pairing has to be screened from the possible candidates for further study. The Niederlinski indices of all of the feed cases and control structures are listed in Table 9. The values of NI are different depending on the control structure or pairing for a given control configuration. The control structures or schemes are defined in parentheses, for example, (L, S), with the left manipulated variable L paired with the upper temperature sensor stage ( $T_U$ ), and the right

**Table 5.** Loop Pairing Results by SVD Analysis of the *L–S* Configuration

	U vector						V vector					
	F1		F2		F3		F1		F2		F3	
M1	-0.081	0.997	0.095	0.996	-0.207	-0.978	-0.048	0.999	-0.297	0.955	0.608	-0.794
	0.997	0.081	0.996	-0.095	-0.978	0.207	-0.999	-0.048	-0.955	-0.297	0.794	0.608
M2	-0.994	-0.111	-1.000	-0.028	0.159	0.987	0.988	-0.152	0.990	-0.138	-0.168	0.986
	-0.111	0.994	-0.028	1.000	0.987	-0.159	0.152	0.988	0.138	0.990	-0.986	-0.168
M3	-0.012	-1.000	-0.001	-1.000	-0.003	-1.000	0.566	-0.825	0.585	-0.811	0.585	-0.811
	-1.000	0.012	-1.000	0.001	-1.000	0.003	0.825	0.566	0.811	0.585	0.811	0.585

**Table 6.** Loop Pairing Results by SVD Analysis of the *L–V* Configuration

	U vector						V vector					
	F1		F2		F3		F1		F2		F3	
M1	-0.749	-0.663	-0.841	-0.542	-0.129	-0.992	0.637	-0.771	0.700	-0.715	0.841	-0.542
	-0.663	0.749	-0.542	0.841	-0.992	0.129	0.771	0.637	-0.715	-0.700	0.542	0.841
M2	-0.997	-0.072	-0.999	0.034	-0.999	-0.049	0.691	-0.723	0.687	-0.727	0.645	-0.764
	-0.072	0.997	0.034	0.999	-0.049	0.999	0.723	0.691	0.727	0.687	0.764	0.645
M3	-0.093	-0.996	-0.027	-0.999	-0.012	-0.999	0.815	-0.580	0.899	-0.437	0.967	-0.257
	-0.996	0.093	-0.999	0.027	-0.999	0.012	0.580	0.815	0.437	0.899	-0.257	-0.967

**Table 7.** Loop Pairing Results by SVD Analysis of the *S–V* Configuration

	U vector						V vector					
	F1		F2		F3		F1		F2		F3	
M1	-0.016	1.000	-0.217	-0.976	0.092	0.996	0.996	0.094	-0.960	-0.282	0.906	0.423
	1.000	0.016	-0.976	0.217	0.996	-0.092	-0.094	0.996	0.282	-0.960	-0.423	0.906
M2	-0.995	-0.098	-1.000	-0.029	-0.984	-0.177	-0.137	-0.991	-0.133	-0.991	-0.177	-0.984
	-0.098	0.995	-0.029	1.000	-0.177	0.984	0.991	-0.137	0.991	-0.133	0.984	-0.177
M3	-0.012	1.000	-0.009	1.000	-0.004	1.000	0.972	0.235	0.944	0.331	0.968	0.253
	1.000	0.012	1.000	0.009	1.000	0.004	-0.235	0.972	-0.331	0.944	-0.253	0.968

**Table 8.** Control Specific Condition Numbers of All Possible Control Configurations

	L–S			L–V			S–V		
	F1	F2	F3	F1	F2	F3	F1	F2	F3
M1	7.16	3.37	3.32	8.10	7.13	655.64	9.89	2.16	4.22
M2	1.68	2.54	1.56	154.83	194.46	218.71	1.78	2.30	1.56
M3	18.24	53.21	110.34	34.78	1069.14	824.64	65.58	86.57	213.32

**Table 9.** Niederlinski Indices of All Possible Control Structures

	(L, S)			(L, V)			(S, V)		
	F1	F2	F3	F1	F2	F3	F1	F2	F3
M1	1.04	1.00	1.03	0.40	-0.83	0.03	42.07	-31.95	35.78
M2	1.00	1.01	0.99	0.17	-0.36	0.17	-338.46	125.86	-163.14
M3	1.28	1.49	1.59	0.54	0.09	-0.43	4.30	2.83	3.66
	(S, L)			(V, L)			(V, S)		
	F1	F2	F3	F1	F2	F3	F1	F2	F3
M1	27.25	-368.64	37.34	-0.67	0.46	-0.03	1.02	0.97	1.03
M2	-352.07	118.56	-193.71	-0.20	0.26	-0.21	1.00	1.01	0.99
M3	4.52	3.03	2.70	-1.16	-0.09	0.30	1.30	1.55	1.38

manipulated variable *S* with the lower temperature sensor stage (*T<sub>L</sub>*).

Possible control schemes for further study were chosen based on the results from the RGA, SVD, CN, and NI analyses. Control structures with either negative NI values or rejected by both the RGA and SVD analyses were first screened from the candidate structures for further study based on the dynamic evaluation. An example of the control-scheme screening procedure for the

F1M1 case is shown in Table 10. Considering the RGA, SVD, CN, and NI analyses, control schemes (L, S), (L, V), and (V, S) were left for the F1M1 case.

Control schemes remaining after screening are listed for the nine feed cases in Table 11. As shown in Table 11, the (L, S) and (V, S) control structures were left for all feed cases. The (L, V) structure remained for all F1 cases and the F2M3, F3M1, and F3M2 cases, and the (V, L) scheme remained for the F2M1,

**Table 10.** Control Scheme Screening for the F1M1 Case

	control scheme candidates					
	(L, S)	(S, L)	(L, V)	(V, L)	(S, V)	(V, S)
RGA	○	✗	○	✗	✗	○
SVD	○	✗	✗	○	✗	○
CN	low	low	low	low	low	low
NI	positive	positive	positive	negative	positive	positive
final decision	○	✗	Δ	✗	✗	○

**Table 11.** Remaining Control Structures after Screening by Steady-State Analyses

	F1	F2	F3
M1	(L, S), (L, V), (V, S)	(L, S), (V, L), (V, S)	(L, S), (L, V), (V, S)
M2	(L, S), (L, V), (V, S)	(L, S), (V, L), (V, S)	(L, S), (L, V), (V, S)
M3	(L, S), (L, V), (V, S)	(L, S), (L, V), (V, S)	(L, S), (V, L), (V, S)

F2M2, and F3M3 cases. The other control structures, such as the (S, L) and (S, V) schemes, were screened out from all feed cases.

Although steady-state analysis is effective for providing insight into control loop pairing with minimum information and quickly screening out the poorest candidates from possible control structures, it cannot take into account the dynamic features of closed-loop systems. Therefore, dynamic analysis is essential for evaluating the closed-loop performance of possible control schemes and finally determining proper control structures. The next section considers dynamic simulations mainly for the remaining control schemes to establish which are suitable for different feed conditions.

## 5. DYNAMIC ANALYSIS FOR EVALUATION OF TWO-POINT TEMPERATURE CONTROL STRUCTURES

The closed-loop dynamic control properties were investigated for the remaining control structure candidates through steady-state analysis. Note that, in addition to the (L, S), (V, S), and (V, L) structures, the (L, V) structure was examined for the F2M1, F2M2, and F3M3 cases despite being screened out in the steady-state analysis. The resulting responses are shown in Figure 5. A 10% increase in feed flow was introduced as a major disturbance. All multiloop proportional–integral–derivative (PID) controllers were tuned by autotune variation.<sup>33</sup> To compare the performances of the three control structures, the settling times and integrals of absolute errors (IAEs) of the closed-loop responses were employed as performance criteria. Tables 12 and 13 list the resulting values of the performance criteria. The settling time and IAE are based on a  $\pm 0.0001$  °C error range of the set point.

In the F1M1 case, the (L, S) control structure showed the best closed-loop performance. The (V, S) configuration showed the largest IAE value of the three candidate structures. In both the F2M1 and F3M1 cases, control behaviors for the candidate structures were quite similar to those in the F1M1 case: The (L, S) structure again showed the fastest settling time and smallest IAE value in the closed-loop response, and the (V, S) configuration gave the largest IAE value. In the F2M1 case, against the prediction from the steady-state analysis result, the (V, L) structure gave even worse performance than the (L, V) structure.

For all M1 cases, the (L, S) structure consistently led to superior control in dynamic states. In the M1 cases, because the ESI value was close to 1 and the separations of A/B and B/C were

easy, the number of stages was relatively small, and thus, the effects of the varying internal liquid flow rate on the temperature changes in the upper and lower stages were rapid. Furthermore, as the results of gain values and SVD analysis indicate, S had little interaction with L because S did not have a significant effect on the temperature of the upper part of the column. The (L, V) structure gave relatively poor performance mainly because of the interaction between L and V from the rectifying role of L and the stripping role of V. For instance, when the reflux and reboiler were on automatic temperature control for  $T_U$  and  $T_L$ , an increase in the feed rate caused an increase in the reflux to reduce  $T_U$ , and the reboiler duty was then increased to control  $T_L$ . In this manner, the control actions counteracted each other, which usually retards quick stabilization. It is also well-known that, in the (L, V) structure, an increase in the reflux rate increases both the tray weir loading and the vapor velocity through the tray deck, which will always push the tray closer to, or even beyond, the point of incipient flooding.<sup>34</sup>

In the (V, S) structure, because V controlled  $T_U$ , control was slower than for the other pairings because of the time taken for the changed internal vapor flow rates to reach the upper stage.

In the F1M2 case, the (L, S) structure gave the fastest settling time and the smallest IAE value. The (L, V) structure also performed reasonably well, whereas the (V, S) structure resulted in the worst closed-loop performance. Because the F1M2 case had an ESI value greater than 1, the feed disturbance did not greatly influence the lower part of the column. Therefore, V varied little to control  $T_L$  because the temperature change of the lower part of the column was small. It was then easy to control  $T_U$  by L. In the F2M2 case, the (L, S) structure provided the best control performance. Note that the (L, V) structure also presented reasonable control performance and even better performance than the (V, S) structure, although it was not selected in the steady-state analysis. On the other hand, the (V, L) structure did not stabilize the system. In the F3M2 case, the (L, S) scheme again showed the best control performance in terms of settling time and IAE value. The (L, V) structure also presented reasonably good control performance for the above-mentioned reason. The (V, S) structure gave the worst performance among the three candidates. These dynamic results show that selection of a control structure by steady-state analysis alone is not sufficient to ensure good dynamic control.

In the M2 cases, where the ESI value was greater than 1, it was easy to control  $T_U$  by L. Therefore, the control structures that paired  $T_U$  with L [such as the (L, S) and (L, V) structures] showed good control performance. Note that the (L, V) structure was not selected in the steady-state analysis for the F2M2 case. The (V, S) configuration was unsuitable for the M2 cases because of the inefficiency in controlling  $T_U$  by V.

For all of the M3 cases, the (V, S) structure consistently produced the best control in dynamic states. The (L, S) structure performed reasonably well. Both the (L, V) and (V, L) structures showed the worst control performance, with significantly poor or

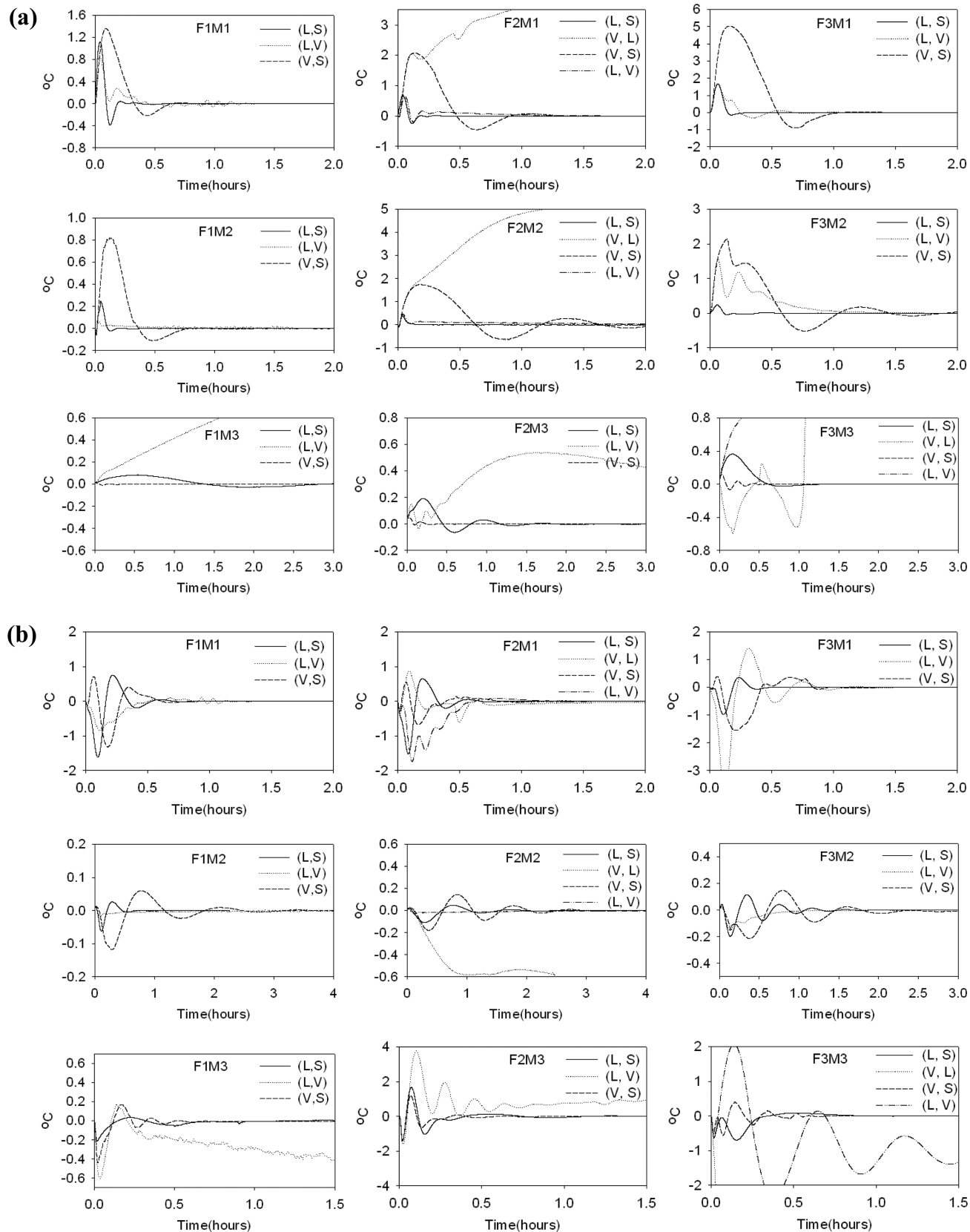


Figure 5. Closed-loop temperature responses of the  $(L, S)$ ,  $(L, V)$ ,  $(V, L)$ , and  $(V, S)$  control structures for the nine feed cases: (a)  $T_U$  and (b)  $T_L$ .

unstable closed-loop responses. In the M3 cases, the ESI value was less than 1, and thus, the effect of a feed disturbance on  $T_U$  was not very significant. In turn, it was easy to control  $T_U$  by manipulating  $V$ . Furthermore, the internal liquid flow rate

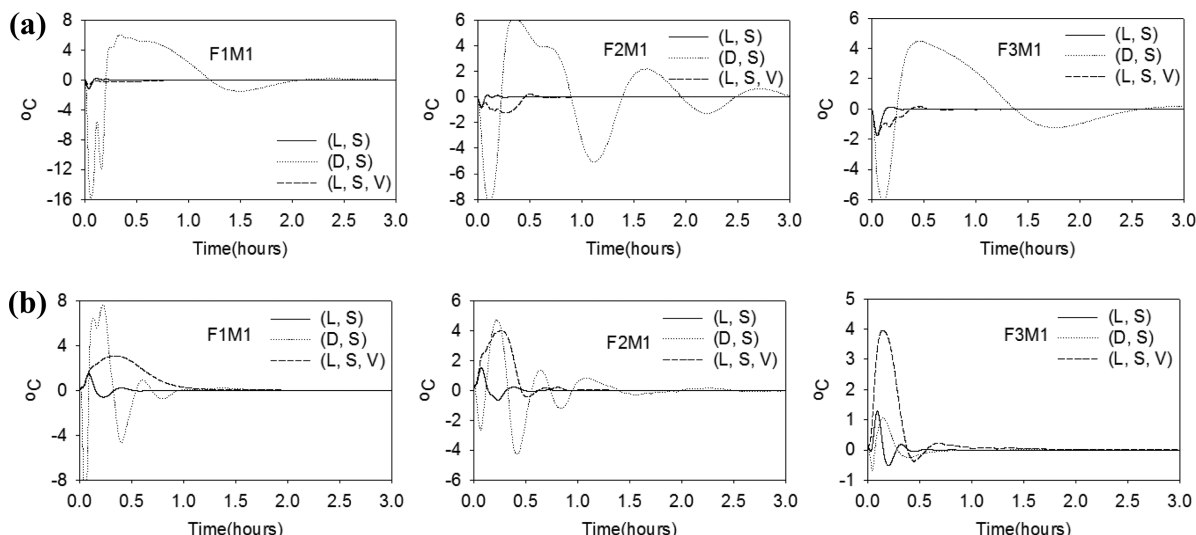
changed by  $S$  allowed a fast response to  $T_L$  because the side draw stage was located in the lower part of the column. For this reason, the  $(V, S)$  structure gave the best control performance of the three control structures. The distance between  $L$  and  $T_U$  was

Table 12. Settling Times (h) of Controlled Stage Temperatures

		(L, S) structure			(L, V) or (L, V)/(V, L) structure			(V, S) structure		
		F1	F2	F3	F1	F2	F3	F1	F2	F3
M1	$T_U$	0.772	0.445	0.489	1.573	2.145/7.233	1.150	1.183	1.822	1.544
	$T_L$	1.272	1.072	0.673	1.517	1.906/5.750	1.973	1.128	1.711	1.467
	total	2.044	1.517	1.162	3.090	4.051/12.983	3.123	2.311	3.533	3.011
M2	$T_U$	0.167	0.490	0.545	0.983	1.573/diverged	2.001	0.773	3.733	1.880
	$T_L$	0.434	1.995	1.472	0.495	2.156/diverged	1.416	2.470	3.450	2.289
	total	0.601	2.485	2.017	1.478	3.729/diverged	3.417	3.243	7.183	4.169
M3	$T_U$	3.495	1.156	1.311	30.144	20.283	22.638/diverged	0.506	0.550	0.783
	$T_L$	0.900	1.834	1.100	20.045	21.178	24.250/diverged	0.683	1.367	0.817
	total	4.395	2.990	2.411	50.189	41.461	46.888/diverged	1.189	1.917	1.600

Table 13. IAEs of Controlled Stage Temperatures

		(L, S) structure			(L, V) or (L, V)/(V, L) structure			(V, S) structure		
		F1	F2	F3	F1	F2	F3	F1	F2	F3
M1	$T_U$	0.091	0.050	0.139	0.111	0.126/27.548	0.265	0.285	0.724	1.906
	$T_L$	0.246	0.225	0.123	0.213	0.443/0.256	0.700	0.254	0.164	0.454
	total	0.317	0.275	0.262	0.324	0.569/27.805	0.965	0.539	0.888	2.360
M2	$T_U$	0.013	0.022	0.025	0.022	0.192/diverged	0.497	0.187	1.430	0.895
	$T_L$	0.011	0.058	0.063	0.006	0.030/diverged	0.051	0.073	0.152	0.168
	total	0.024	0.080	0.088	0.028	0.222/diverged	0.548	0.260	1.582	1.063
M3	$T_U$	0.107	0.080	0.130	11.99	2.767	9.691/diverged	0.001	0.005	0.015
	$T_L$	0.035	0.269	0.135	6.199	5.334	5.352/diverged	0.048	0.150	0.086
	total	0.142	0.349	0.265	18.189	8.101	15.043/diverged	0.049	0.155	0.101

Figure 6. Closed-loop temperature responses of the (L, S), (D, S), and (L, S, V) control structures for the F1M1, F2M1, and F3M1 cases: (a)  $T_U$  and (b)  $T_L$ .

larger than in the M1 and M2 cases, which made it difficult to control  $T_U$  by manipulating  $L$  and, in turn, caused performance degradation of the (L, V) structure.

## 6. COMPARISON WITH OTHER CONTROL SCHEMES: (L, S, V) AND (D, S) STRUCTURES

In this section, the (L, S) control structure is compared with the (L, S, V) control structure for the M1 cases to evaluate the control performance between the two- and three-point temperature controls. Kiss and Bildea<sup>35</sup> studied three-point control structures for a DWC. In their work, the studied feed was composed of 20% *n*-pentane, 60% *n*-hexane, and 20% *n*-heptane, which is exactly same as the F3M1 case used in this study, and the

(L, S, V) control structure was suggested as the best structure to handle persistent disturbances in reasonably short times.

For this comparison, the specifications of product mole fraction were selected as 0.99, 0.94, and 0.99 for the distillate, intermediate, and bottom products, respectively. DWC structures were employed with those listed in Table 2 for each corresponding M1 case. In the (L, S, V) structure, S controls the temperature of the stage below the side draw stage ( $T_S$ ), whereas L and V control  $T_U$  and  $T_L$ , respectively. Sensor locations for the (L, V) structure in Table 3 were used for  $T_U$  and  $T_L$  in the (L, S, V) structure. A 10% decrease in feed flow was introduced as a major disturbance. All multiloop PID controllers were tuned by autotune variation.<sup>33</sup>

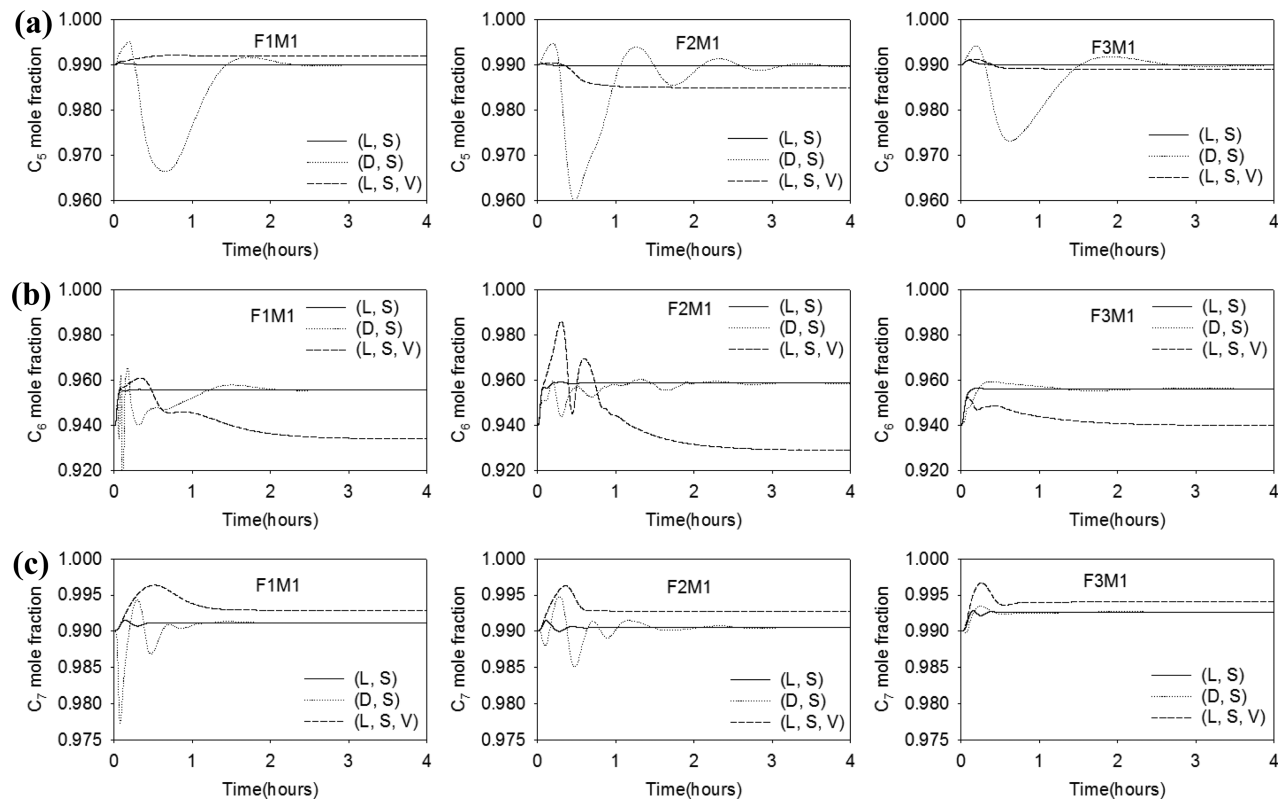


**Figure 7.** Closed-loop composition responses of the  $(L, S)$ ,  $(D, S)$ , and  $(L, S, V)$  control structures for the F1M1, F2M1, and F3M1 cases: (a) *n*-pentane in the distillate product, (b) *n*-hexane in the intermediate product, and (c) *n*-heptane in the bottom product.

The closed-loop temperature responses are shown in Figure 6. As seen from the responses, the two-point control quickly settled the disturbance for all M1 cases, with lower integrated errors compared with the three-point control. In the  $(L, S, V)$  control structure, the interaction mechanism between  $S$  and  $V$  was similar to that between  $L$  and  $V$ .<sup>34</sup> Any control action by  $L$ ,  $S$ , or  $V$  interacted with the others, which inherently led to a longer settling time than obtained by two-point control with the  $(L, S)$  structure. The resulting composition responses are also shown in Figure 7. The two-point temperature control by the  $(L, S)$  structure apparently provided a faster settling time in composition responses with less overshoot and interaction than the three-point control. The composition offsets of the distillate and bottom products obtained by the  $(L, S)$  structure remained within a reasonably narrow range ( $\pm 0.27\%$ ) and even smaller than those obtained by the  $(L, S, V)$  structure. However, the three-point control of the  $(L, S, V)$  structure provided relatively small composition offsets of the intermediate product because  $T_S$  was controlled directly: In the  $(L, S, V)$  structure, the largest offset of the intermediate product was about  $-1.2\%$  through all M1 cases whereas that obtained by the  $(L, S)$  structure ranged from about 1.7 to 2.0%.

If automatic regulation of the material balance is not considered in the manual mode, then  $D$  and  $B$  can also be possible candidates for manipulate variables for temperature control. The  $(D, S)$  control structure was also examined as an alternative to the  $(L, S)$  structure. The results are also included in Figures 6 and 7. Note that the bottom level control with  $V$  (accordingly, control of  $T_L$  by  $B$ ) was excluded because of its impracticality with several critical limitations such as slow dynamics and inverse responses. As seen from Figures 6 and 7, the  $(D, S)$  structure showed the worst transient responses among

the compared three structures. These sluggish and oscillatory responses seem to be due to its strong interactions by the manipulation actions of  $L$  for receiver level control and  $V$  for temperature control.

## 7. CONCLUSIONS

In this work, the generalized properties of two-point temperature control for DWCs were analyzed in connection with the feed characteristics. Steady-state analyses such as steady-state gain values, SVD, RGA, CN, and NI were investigated to select the best sensor locations and screen out poor control structures. SVD analysis turned out to be effective in finding proper sensor locations, particularly in the upper stages for the M3 cases, which were unclear in the steady-state gain matrix. It was observed that most of the sensitive stages in temperature changes, relevant to control, were commonly located around the end of the dividing-wall section. The  $(L, S)$  and  $(V, S)$  control structures were recommended through the steady-state analyses for all feed cases, and the  $(L, V)$  structure was suitable for all of the feed cases except F2M1, F2M2, and F3M3, for which the  $(V, L)$  structure was suggested.

The closed-loop dynamic control properties were investigated for the  $(L, S)$ ,  $(V, S)$ , and  $(L, V)$  control structures for all feed cases, and the  $(V, L)$  structure was also investigated for the F2M1, F2M2, and F3M3 cases. The dynamic analysis revealed that the best control structure was closely related to the relative volatility characteristics (e.g., the ESI value) in the feed mixture. The tendency of the proper control structure was independent of the feed composition for a given mixture. When the ESI value of the feed mixture was close to 1 (the M1 cases) or large (the M2 cases), the  $(L, S)$  control structure gave the best control performance. The  $(L, S)$  control structure also provided

reasonable performance when the ESI value was small (the M3 cases). On the other hand, when the ESI value was small (the M3 cases), the (V, S) pairing structure resulted in the best control performance with the fastest closed-loop response and the smallest IAE value. The (L, V) structure, which is popular in conventional distillation columns, resulted in the worst control performance, with significantly poorer closed-loop responses for the M3 cases, but still gave reasonable performance in the M2 cases. The (V, L) structure gave the worst responses, which were even unstable, because of its dynamic characteristics, although it passed the steady-state screening for several feed cases. In conclusion, for the two-point temperature control of DWCs, the (L, S) control structure is preferentially recommended for the M1 and M2 cases, and the (V, S) structure is recommended for the M3 case.

To evaluate the control performance between the two- and three-point temperature controls, the (L, S) structure was compared with the (L, S, V) structure for the M1 cases. Two-point control by the (L, S) structure consistently provided more stable and faster responses with less offset of the distillate and bottom product purities, although it gave larger offset of the intermediate product purity than the three-point control by the (L, S, V) structure. If composition offsets within a reasonable range are allowed, two-point temperature control can be an attractive control scheme for a DWC. Two-point control by the (D, S) structure was also examined, but it showed poor transient responses because of strong loop interactions.

## ■ ASSOCIATED CONTENT

### Supporting Information

(1) Controller tuning parameters for all two-point control structures studied; (2) the settling times and IAE values for the (L, S), (D, S), and (L, S, V) structures; and (3) U vector plots of the L-V and S-V configurations. This material is available free of charge via the Internet at <http://pubs.acs.org>.

## ■ AUTHOR INFORMATION

### Corresponding Author

\*E-mail: mynlee@yu.ac.kr (M.L.), sunwon@kaist.ac.kr (S.P.).

### Notes

The authors declare no competing financial interest.

## ■ ACKNOWLEDGMENTS

This research was supported by Basic Science Research Program through the National Research Foundation of Korea (NRF) funded by the Ministry of Education, Science and Technology (2012012532).

## ■ REFERENCES

- Fidkowski, Z.; Krolikowski, L. Energy Requirements of Non-conventional Distillation Systems. *AIChE J.* **1990**, *36*, 1275–1278.
- Hernández, S.; Jiménez, A. Design of Energy-Efficient Petlyuk Systems. *Comput. Chem. Eng.* **1999**, *23*, 1005–1010.
- Jiménez, A.; Ramírez, N.; Castro, A.; Hernández, S. Design and Energy Performance of Alternative Schemes to the Petlyuk Distillation System. *Trans. Inst. Chem. Eng.* **2003**, *81* (AS), 518–524.
- Halverson, I. J.; Skogestad, S. Minimum Energy Consumption in Multicomponent Distillation. 2. Three-Product Petlyuk Arrangements. *Ind. Eng. Chem. Res.* **2003**, *42*, 605–615.
- Halverson, I. J.; Skogestad, S. Shortcut Analysis of Optimal Operation of Petlyuk Distillation. *Ind. Eng. Chem. Res.* **2004**, *43*, 3994–3999.
- Aspirón, N.; Kaibel, G. Dividing Wall Columns: Fundamentals and Recent Advances. *Chem. Eng. Process.* **2010**, *49*, 139–146.
- Long, N.; Lee, S.; Lee, M. Design and Optimization of a Dividing Wall Column for Debottlenecking of the Acetic Acid Purification Process. *Chem. Eng. Process.* **2010**, *49*, 825–835.
- Long, N.; Lee, M. Improved Energy Efficiency in Debottlenecking Using a Fully Thermally Coupled Distillation Column. *Asia-Pac. J. Chem. Eng.* **2011**, *6*, 338–348.
- Shin, J.; Lee, S.; Lee, J.; Lee, M. Manage Risks with Dividing-Wall Column Installations. *Hydrocarbon Process.* **2011**, *90*, 59–62.
- Long, N.; Lee, M. Improvement of the Deethanizing and Depropanizing Fractionation Steps in NGL Recovery Process Using Dividing Wall Column. *J. Chem. Eng. Jpn.* **2012**, *45* (4), 1–10.
- Wright, R. O. *Fractionation Apparatus*. U.S. Patent 2,471,134, 1949.
- Kaibel, G.; Schoenmakers, H. Process Synthesis and Design in Industrial Practice. *Proc. ESCAPE-12* **2002**, 9.
- Agrawal, R.; Fidkowski, Z. T. Are Thermally Coupled Distillation Columns Always Thermodynamically More Efficient for Ternary Distillations? *Ind. Eng. Chem. Res.* **1998**, *37*, 3444–3454.
- Wolff, E. A.; Skogestad, S. Operation of Integrated Three-Product (Petlyuk) Distillation Columns. *Ind. Eng. Chem. Res.* **1995**, *34*, 2094–2103.
- Annakou; Meszaros, A.; Fonyo, Z.; Mizsey, P. Operability Investigation of Energy Integrated Distillation Schemes. *Hung. J. Ind. Chem.* **1996**, *24*, 155–160.
- Mutalib, M. I. A.; Smith, R. Operation and Control of Dividing Wall Distillation Columns: Part 1. *Trans. Inst. Chem. Eng.* **1998**, *76*, 308–318.
- Hernández, S.; Jiménez, A. Controllability Analysis of Thermally Coupled Distillation Systems. *Ind. Eng. Chem. Res.* **1999**, *38*, 3957–3963.
- Serra, M.; Perrier, M.; Espuna, A.; Puigjaner, L. Analysis of Different Control Possibilities for the Divided Wall Column: Feedback Diagonal and Dynamic Matrix Control. *Comput. Chem. Eng.* **2001**, *25*, 859–866.
- Adrian, T.; Schoenmakers, H.; Boll, M. Model Predictive Control of Integrated Unit Operations: Control of A Divided Wall Column. *Chem. Eng. Process.* **2004**, *43*, 347–355.
- Segovia-Hernández, J. G.; Hernández, S.; Ramírez, V. R.; Jiménez, A. A Comparison of the Feedback Control Behavior Between Thermally Coupled and Conventional Distillation Schemes. *Comput. Chem. Eng.* **2004**, *28*, 811–819.
- Cho, Y.; Kim, B.; Kim, D.; Han, M.; Lee, M. Operation of Divided Wall Column with Vapor Sidedraw Using Profile Position Control. *J. Process Control.* **2009**, *19*, 932–941.
- Mutalib, M. I. A.; Smith, R. Operation and Control of Dividing Wall Distillation Columns: Part 2. *Trans. Inst. Chem. Eng.* **1998**, *76*, 319–334.
- Joseph, B.; Brosilow, C. B. Inferential Control of Processes: Part I. Steady State Analysis and Design. *AIChE J.* **1978**, *24*, 485–492.
- Fidkowski, Z.; Krolikowski, L. Minimum Energy Requirements of Thermally Coupled Distillation Systems. *AIChE J.* **1987**, *33*, 643–653.
- Yu, C. C.; Luyben, W. L. Use of Multiple Temperatures for the Control of Multicomponent Distillation Columns. *Ind. Eng. Chem. Res.* **1984**, *23*, 590–597.
- Lee, S.; Shamsuzzoha, M.; Han, M.; Kim, Y.; Lee, M. Study of the Structural Characteristics of a Divided Wall Column Using The Sloppy Distillation Arrangement. *Korean J. Chem. Eng.* **2011**, *28*, 348–356.
- Tedder, D. W.; Rudd, D. F. Parametric Studies in Industrial Distillation. Part I. Design Comparisons. *AIChE J.* **1978**, *24*, 303–315.
- Kister, H. Z. *Distillation Operation*; McGraw-Hill: New York, 1990.
- Moore, C. F. Selection of Controlled and Manipulated Variables. *Practical Distillation Control*; Luyben, W. L., Ed.; Van Nostrand Reinhold: New York, Chapter 8, 1992; pp 140–177.
- Bristol, E. H. On a New Measure of Interaction for Multivariable Process Control. *IEEE Trans. Autom. Control* **1966**, AC-11, 133–134.
- Deshpande, P. B. *Multivariable Process Control*; Instrument Society of America: Research Triangle Park, NC, 1989.

- (32) Niederlinski, A. A Heuristic Approach to the Design of Linear Multivariable Control System. *Automatica* **1971**, *7*, 691–701.
- (33) Astrom, K. J.; Hagglund, T. A Frequency Domain Method for Automatic Tuning of Simple Feedback Loops. *Proceedings of the 23rd Conference on Decision and Control*; IEEE: Las Vegas, NV, 1984; pp 299–304.
- (34) Lieberman, N. P.; Lieberman, E. T. *Working Guide to Process Equipment*, 2nd ed.; McGraw-Hill: New York, 2003.
- (35) Kiss, A. A.; Bildea, C. S. A Control Perspective on Process Intensification in Dividing-Wall Columns. *Chem. Eng. Process.* **2011**, *50*, 281–292.